Thermodynamic cycles with nearly universal maximum-work efficiencies

1989 J. Phys. A: Math. Gen. 22 4019

(http://iopscience.iop.org/0305-4470/22/18/034)

J. Phys. A: Math. Gen. 22 (1989) 4019-4026. Printed in the UK

Thermodynamic cycles with nearly universal maximum-work efficiencies

Peter T Landsberg† and Harvey S Leff‡

† Faculty of Mathematical Studies, University of Southampton, Southampton SO9 5NH, UK

‡ Physics Department, California State Polytechnic University, Pomona, CA 91768, USA

Received 7 March 1989

Abstract. Important thermodynamic heat engine cycles can be regarded as special cases of a more universal 'generalised' cycle. For specific choices of a continuously variable parameter, this generalised cycle reduces to the Carnot, Otto, Joule-Brayton, Diesel and other known cycles. Of particular interest is the thermal efficiency when characteristic temperatures between the highest and lowest operating temperatures (T_+ and T_-) are chosen to maximise the work output per cycle. This maximum-work efficiency is found to be equal to, or to be well approximated by, the Curzon-Ahlborn efficiency, $\eta_{CA} \equiv 1-(T_-/T_+)^{1/2}$ for a broad spectrum of cycles and temperatures. The generalised cycle, characterised by two adiabatics and two heat transfer paths with constant heat capacities, sheds light on this remarkable and important, but largely unknown, property.

1. Introduction

The study of heat engines is central to the development and understanding of thermodynamics. One of the most commonly used corollaries of the second law of thermodynamics is Carnot's principle: a reversible Carnot cycle, operating between fixed reservoir temperatures T_+ and $T_- < T_+$, has the highest thermal efficiency

$$\eta_C = 1 - T_-/T_+ \tag{1.1}$$

possible for such operation. Reversible cycles, such as the Otto, Diesel and Joule-Brayton cycles (see, e.g., [1]), serve as models for real heat engines. Historically, these cycles have been examined separately, their most obvious common feature being that their efficiencies do not exceed η_C.

Recently, several reversible heat engines were examined under conditions of maximum work production per cycle [2]. Surprisingly, it was found that they share the property that their maximum-work efficiencies are all either equal to or well approximated by

$$\eta_{CA} = 1-(T_-/T_+)^{1/2} \tag{1.2}$$

where T_+ and T_- are the maximum and minimum cycle temperatures. This efficiency applies also to the Curzon-Ahlborn irreversible heat engine operating between reservoirs at temperatures T_- and T_+ under maximum power conditions, and obeying a linear heat transfer law [3].

0305-4470/89/184019+08$02.50

The remarkable 'near-universality' of η_{CA} is the impetus for studying a generalised cycle that encompasses all those noted above. This study is not unduly academic, for first- and second-law efficiencies of power plants are reasonably consistent wtih (1.2) [3, 4]. The universal nature of η_{CA} is an important new finding in the old subject of thermodynamics. The present study is intended to elaborate upon it, illustrating the extent to which the maximum-work efficiency is well approximated by (1.2) for a broad spectrum of cycles and temperatures.

2. A thermodynamic cycle with interesting properties

Consider a reversible cycle consisting of two adiabatics and two segements with constant heat capacity $C > 0$ of the working fluid, as depicted in figure 1. The maximum and minimum cycle temperatures are T_+ and T_-. Along the heating and cooling segments, the temperature varies from T to T_+ and from T' to T_-, respectively. The heat transfers to the fluid, which are accomplished via an appropriate sequence of heat reservoirs, are

$$Q_{\text{in}} = C(T_+ - T) \geqslant 0 \tag{2.1a}$$

$$Q_{\text{out}} = C(T_- - T') \leqslant 0. \tag{2.1b}$$

The adjustable temperatures T and T' are coupled because the fluid's entropy change per cycle is zero, i.e. $\Delta S = C[\ln(T_+/T) + \ln(T_-/T')] = 0$ or

$$T' = T_- T_+ / T. \tag{2.2}$$

The work done per cycle is

$$W = Q_{\text{in}} + Q_{\text{out}} = C(T_+ - T + T_- - T_- T_+ / T). \tag{2.3}$$

What values T^* of T and T'^* of T' maximise W for fixed T_+ and T_-? Defining $\tau \equiv T_-/T_+$, the maximum work W^* is obtained when

$$T^* = T'^* = (T_- T_+)^{1/2} = T_+ \tau^{1/2} \tag{2.4}$$

whence

$$W^* = CT_+(1 - \tau^{1/2})^2 \tag{2.5}$$

$$Q^*_{\text{in}} = CT_+(1 - \tau^{1/2}) \tag{2.6}$$

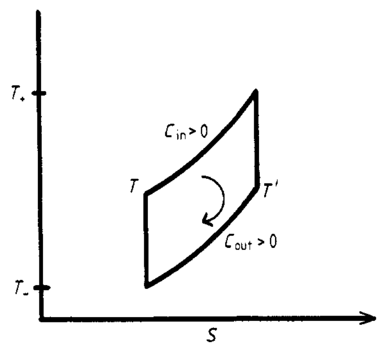

Figure 1. Temperature-entropy diagram of a reversible cyle with two adiabatic (constant entropy) segments and two paths with equal constant heat capacities, $C_{\text{in}} = C_{\text{out}} \equiv C > 0$.

and

$$\eta^* = W^*/Q_{\text{in}}^* = 1-\tau^{1/2} = \eta_{\text{CA}}. \tag{2.7}$$

This maximum-work approach is clearly a rather simple way of obtaining η_{CA}.

In general, the efficiency $\eta = W/Q_{\text{in}}$ depends on T_-, T_+ and T, and is

$$\eta = \frac{C(T_+ - T)(1 - T_-/T)}{C(T_+ - T)} = 1 - (T_+/T)\tau \tag{2.8}$$

whence

$$\frac{T}{T_+} = \frac{\tau}{1-\eta}. \tag{2.9}$$

If one now defines a 'reduced' heat input q and a 'reduced' efficiency e via

$$q \equiv \frac{Q_{\text{in}}}{C(T_+ - T_-)} \tag{2.10a}$$

$$e \equiv \frac{\eta}{\eta_c} = \frac{\eta}{1-\tau} \tag{2.10b}$$

one finds, using (2.1) and (2.9), that

$$q = \frac{1-e}{1-e\eta_C}. \tag{2.11}$$

This relation is shown in figure 2 for $\tau = 0.1$, 0.3 and 0.9.

Examination of (2.1), (2.3) and (2.8) shows that $q = 0$ at $e = 1$, which corresponds to $T = T_+$ and $W = 0$; and $q = 1$ at $e = 0$, which occurs when $T = T_-$ and $W = 0$. Between these two zeros of W there must lie a maximum. Using (2.7) to obtain e^*, one finds

$$q^* = e^* = \frac{(1-\tau^{1/2})}{(1-\tau)} = (1+\tau^{1/2})^{-1}. \tag{2.12}$$

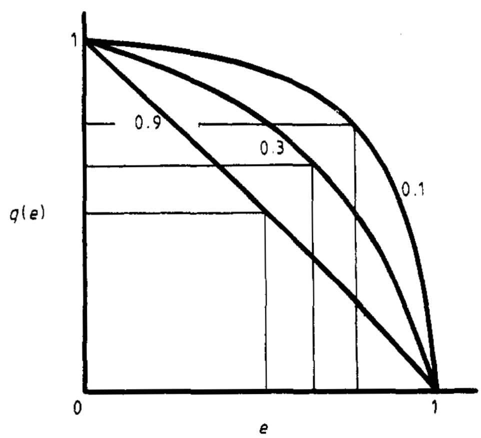

Figure 2. The reduced heat input (2.10a) plotted against the reduced efficiency (2.10b). Three curves are shown, corresponding to $\tau = 0.1$, 0.3 and 0.9. In each case, the reduced efficiency at maximum work is shown by the appropriate side of the maximum-area inscribed rectangle (which turns out to be a square).

Therefore, on the q–e diagram the maximum-work point lies at (e^*, q^*) with $q^* = e^*$. The line from 0 at 45° intersects the curve at the maximum-work point. The rectangular areas (for $\tau = 0.1$, 0.3, 0.9) shown in figure 2 each have the value

$$(e^*)^2 = \frac{W^*}{CT_+\eta_C^2} = (1+\tau^{1/2})^{-2} \tag{2.13}$$

which is proportional to the maximum work output, W^*.

The q–e diagram, with the appropriate inscribed rectangle representing the maximum work output, is familar from solar cell analyses where one uses a current-voltage relation, and the product of the two coordinates represents power. This heat current-efficiency representation follows an idea used for endoreversible heat engines by de Vos [5].

The cycle described here corresponds to the Otto cycle if $C = C_v$ and to the Joule–Brayton cycle if $C = C_p$ [2]. The properties represented in (2.7) and figure 2 make this cycle elegant and interesting. The generalised cycle introduced in the next section shares these features, and underscores the importance of η_{CA}.

3. Generalisations

Consider now a generalisation in which the heat capacities along the heat transfer paths are still constants, called C_{in} and C_{out}, but with no restriction on their relative magnitudes or algebraic signs†. Equations (2.1a) and (2.1b) are then replaced by

$$Q_{in} = |C_{in}|(T_+ - T) \geqslant 0 \tag{3.1a}$$

$$Q_{out} = |C_{out}|(T_- - T') \leqslant 0. \tag{3.1b}$$

For the *special* case where $|C_{in}| = |C_{out}| \equiv C$, the cycles in figures 3(a)–(c) also become possible, and the analysis in § 2 is still valid. For any path (labelled h) with heat capacity C_h, $\mathrm{d}T/\mathrm{d}S = T/C_h$, and hence the paths shown in figure 3 with $\mathrm{d}T/\mathrm{d}S < 0$ have negative heat capacities. Notice that (2.2) implies that the variable temperatures, T and T', in figures 1 and 3(a)–(c) can range from T_- to T_+.

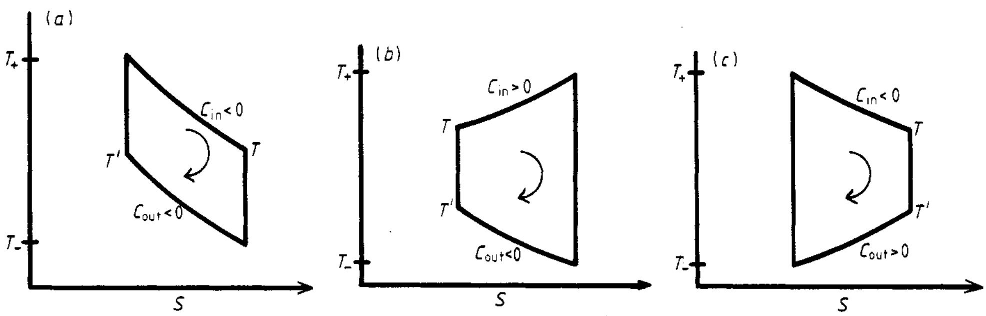

Figure 3. Temperature–entropy diagram of three reversible cycles that are generalisations of the cycle in figure 1: (a) $C_{in} = C_{out} < 0$; (b) $C_{in} > 0$, $C_{out} < 0$, with $|C_{in}| = |C_{out}|$; (c) $C_{in} < 0$, $C_{out} > 0$, with $|C_{in}| = |C_{out}|$.

† Although it is not widely appreciated, negative heat capacities are common along certain types of paths; e.g. an ideal gas has negative heat capacity along so-called polytropic paths described by pV^n = constant, with $1 < n < \gamma \equiv C_p/C_v$. See [6].

More generally, $|C_{in}|$ and $|C_{out}|$ are not necessarily equal, and a new analysis, paralleling that in § 2, is needed. The ratio parameter

$$\theta \equiv |C_{in}|/|C_{out}| \qquad \theta > 0 \tag{3.2}$$

is helpful in categorising the generalised cycles. Table 1 lists four well known special cases, for which the heat capacities are defined to be positive, and gives the θ value for each.

Analysis of the generalised cycle with arbitrary positive θ is straightforward. Key results, which are extensions of the equations in § 2, are summarised in table 2, and results for several interesting limiting values of θ are tabulated in table 3. The extension of (2.2) in table 2 has the consequence that either T or T' is restricted to a subset of $[T_-, T_+]$ when $\theta \neq 1$. This is shown clearly in the plot of T' against T for five values

Table 1. Parameter choices for common reversible heat engine cycles.

Cycle	Q_{in} segment	Q_{out} segment	C_{in}	C_{out}	θ
Otto	isochore	isochore	C_v	C_v	1
Joule-Brayton	isobar	isobar	C_p	C_p	1
Diesel[a]	isobar	isochore	C_p	C_v	γ
Atkinson[a]	isochore	isobar	C_v	C_p	γ^{-1}

[a] For a dilute diatomic gas working fluid, $\gamma = C_p/C_v = \frac{7}{2}/\frac{5}{2} = 1.40$ and $\gamma^{-1} = 0.71$; for polyatomic gases, $\gamma = \frac{8}{2}/\frac{6}{2} = 1.33$ and $\gamma^{-1} = 0.75$.

Table 2. Generalisations of equations from § 2 for $\theta \neq 1$[a].

Equation number	Generalisation
(2.2)	$T' = T_-(T_+/T)^\theta$
(2.3)	$W = |C_{out}|[\theta(T_+ - T) + T_- - T_-(T_+/T)^\theta]$
(2.4)	$T^* = T'^* = (T_- T_+^\theta)^{1/(\theta+1)}$
(2.7)	$\eta^*(\theta, \tau) = 1 - \theta^{-1}(\tau^{1/(\theta+1)} - \tau)/(1 - \tau^{1/(\theta+1)})$
(2.8)	$\eta(\theta, T_+, T_-, T) = 1 + (T_-/T_+)[1 - (T_+/T)^\theta]\{\theta[1 - T/T_+]\}^{-1}$

[a] $\tau \equiv T_-/T_+$

Table 3. η^* for various choices of θ[a].

θ	η^*	Comment
1	$1 - \tau^{1/2}$	Otto, Joule-Brayton, and Curzon-Ahlborn cycles [2, 3]
0	$1 + \tau(1-\tau)^{-1}\ln(\tau)$	Finite heat source and infinite sink [7, 8]
∞	$1 + (1-\tau)/\ln(\tau)$	Finite heat sink and infinite source [7].
$1/\gamma$	$1 + (\tau - \tau^f)/[(1-f)(1-\tau^f)]$	$f \equiv \gamma/(1+\gamma)$; $C_{in} = C_v$; $C_{out} = C_p$ Atkinson cycle with ideal gas working fluid [2]
γ	$1 + f(\tau - \tau^f)/[(1-f)(1-\tau^f)]$	$f \equiv 1/(1+\gamma)$; $C_{in} = C_p$; $C_{out} = C_v$ Diesel cycle with ideal gas working fluid [2]

[a] $\tau \equiv T_-/T_+$ and $\gamma \equiv C_p/C_v$

of θ between 0.2 and 10 in figure 4. When $\theta > 1$, $T > T_{\min} > T_-$; when $\theta < 1$, $T' < T'_{\max} < T_+$. The temperatures $T_{\min}$ and $T'_{\max}$ depend upon θ. Only for the special case $\theta = 1$ can both T and T' span the full interval $[T_-, T_+]$†.

The reason for the limited range of T is illustrated for the special case $\theta > 1$ and $C_{in} > C_{out} > 0$ in figure 5. As the intermediate temperature T in figure 5(a) is reduced, T' must increase. T' reaches T_+ (figure 5(b)) *before* T has reached T_- because $C_{in} > C_{out}$ implies that $(\mathrm{d}T/\mathrm{d}S)_{out} > (\mathrm{d}T/\mathrm{d}S)_{in}$. Hence, T cannot get smaller than its value in figure 5(b). Similar illustrative graphs can be made for other choices of C_{in} and C_{out}.

The restricted ranges of T or T' when $\theta \neq 1$ limit the range of possible thermal efficiencies for these generalised cycles. This is illustrated in figure 6, which shows the reduced heat input $q \equiv Q_{in}/|C_{in}|(T_+ - T_-)$ as a function of the reduced efficiency e for five values of θ when $\tau = 0.3$. For $\theta = 1$, the curve is identical to the curve for $\tau = 0.3$ in figure 2. For *any* θ, the Carnot reduced efficiency of unity is possible in the limit of zero heat input, which of course, results in zero work output. In this limit, the two adiabatics approach one another, and the generalised cycle with any value of θ effectively becomes a Carnot cycle.

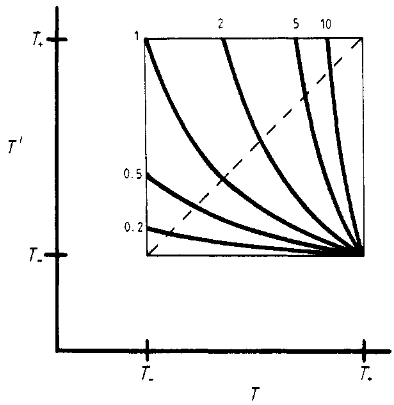

Figure 4. T' plotted against T, as given in the generalisation of (2.2), table 2. Curves are shown for $\theta = 0.2, 0.5, 1, 2, 5$ and 10, with T and T' restricted to (T_-, T_+). The broken line is $T' = T$.

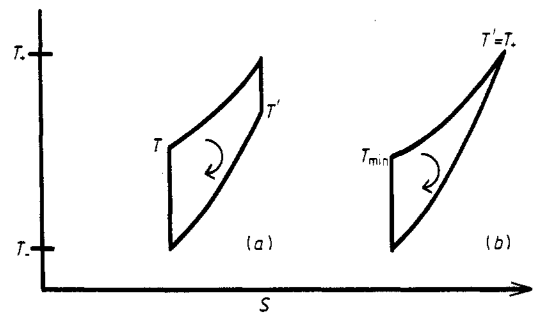

Figure 5. Temperature-entropy diagram of a reversible cycle with $C_{in} > C_{out} > 0$; i.e. $\theta \equiv |C_{in}|/|C_{out}| > 0$, for two different choices of T and T': (a) $T_- < T_{\min}(\theta) < T < T' < T_+$; ($b$) $T = T_{\min}(\theta) < T' = T_+$.

† When the heat capacities along the upper and lower branches have opposite algebraic signs, those two branches intersect when $T < T'$, giving double-looped cycles. These are relatively inefficient, and are of academic interest only.

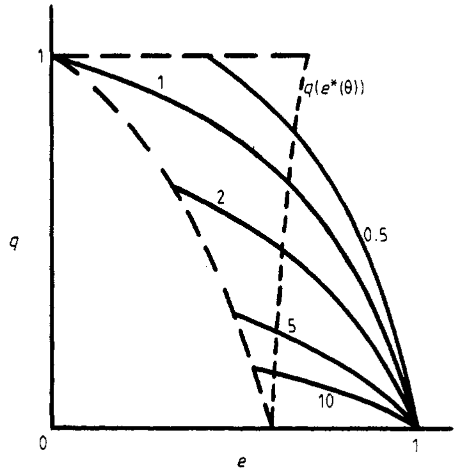

Figure 6. The reduced heat input q plotted against reduced efficiency e for $\theta = 0.5$, 1, 2, 5 and 10, with $\tau = 0.3$. The short-dashed curve is $q(e^*(\theta))$, for $0 < \theta < \infty$. The fact that it is nearly vertical indicates that e^* varies relatively little under large changes in θ. The long-dashed curve is $q(e_-)$ where e_- (a function of θ) is the *minimum* possible reduced efficiency. For $\theta > 1$ this non-zero minimum occurs because T has a minimum *above* T_-; for $\theta < 1$ it occurs because T' is restricted to values *below* T_+. The restrictions on T and T' are evident in figure 4. When $\theta = 1$, both T and T' can vary from T_- to T_+ and the minimum efficiency $e_- = 0$.

4. Near-universality

The most interesting feature of the generalised cycle is the degree to which its maximum-work efficiency $\eta^*(\theta, \tau)$ (table 3) is well approximated by the Curzon–Ahlborn efficiency, η_{CA}, for a broad spectrum of θ and τ values. This is illustrated graphically in figure 6 by the large slope of $q(e^*(\theta))$, the locus of maximum-work points. Specifically, as shown in figure 7, the difference between η^* and η_{CA} never exceeds 14%.

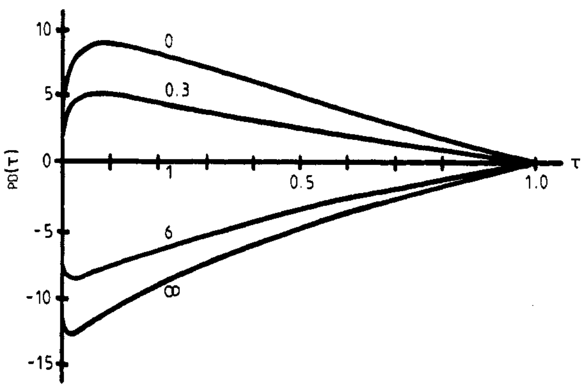

Figure 7. Percent difference, $\text{PD}(\tau) \equiv 100 \times [\eta^*(\tau, \theta) - \eta^*(\tau, 1)]/\eta^*(\tau, 1)$, plotted against τ. Curves are shown for $\theta \to 0$, 0.3, 1, 6 and ∞. The magnitude of $\text{PD}(\tau)$ is under 14% for $0 \leq \tau < \infty$.

References

[1] Crawford F H 1963 *Heat, Thermodynamics, and Statistical Physics* (New York: Harcourt, Brace, and World) ch 8
[2] Leff H S 1987 *Am. J. Phys.* **55** 602–10
[3] Curzon F and Ahlborn B 1975 *Am. J. Phys.* **43** 22–4
[4] Bejan A 1988 *Int. J. Heat Mass Transfer* **31** 1211–9
[5] De Vos A 1987 *J. Phys. D: Appl. Phys.* **20** 232–6
[6] Landsberg P T 1961 *Thermodynamics* (New York: Interscience) p 42, 45
[7] Leff H S 1987 *Am. J. Phys.* **55** 701–5
[8] Ondrechen M J, Andresen B, Mozurkewich M and Berry R S 1981 *Am. J. Phys.* **49** 681–5